Neutron diffraction study of the magnetic order in the $Dy(Mn_{1-x}Al_x)_2$ system in the region of a magnetic instability

I. V. Golosovsky
St. Petersburg Nuclear Physics Institute, 188350 Gatchina, St. Petersburg, Russia

I. Mirebeau
Laboratoire Léon Brillouin, CE-Saclay, F-91191 Gif-sur-Yvette, France

A. S. Markosyan
Faculty of Physics, M. Lomonosov Moscow State University, 119899 Moscow, Russia

P. Fischer and V. Yu. Pomjakushin
Laboratory of Neutron Scattering, ETHZ & PSI, CH-5232 Villigen PSI, Switzerland
(Received 20 April 2001; published 29 November 2001)

Neutron diffraction study of $Dy(Mn_{1-x}Al_x)_2$ shows that with substituting Mn by Al the magnetic system goes through the instability region. At small substitution, phases with intrinsic and induced Mn spins coexist. With increasing Al content the long-range order of Dy and induced Mn moments is progressively suppressed while a short-range magnetic order of intrinsic Mn spins develops. A small substitution destroys the ferromagnetic component of the Dy moment and magnetic order transforms from a canted to a collinear one. Using a Heisenberg model with nearest-neighbors interactions applied to the ''sandwich'' type of magnetic order in $DyMn_2$, one can explain this transformation. It provides a ratio of Dy-Dy and Dy-Mn exchange interactions equal to 0.26(1).

DOI: 10.1103/PhysRevB.65.014405 PACS number(s): 75.25.+z, 71.20.Lp

I. INTRODUCTION

The Laves phase compounds RMn_2, where R stands for a rare-earth element, present an original series of magnetic materials whose properties are governed by magnetic instability and geometrical frustration in the Mn sublattice.[1,2] In these compounds the character of magnetic $3d$ electrons can be changed between itinerant and localized, when the temperature, pressure or composition is varied.[3–9]

The magnetic instability of Mn was explained by the existence of a critical Mn-Mn interatomic distance of about 2.7 Å above which $3d$ electrons exhibit a sudden localization of magnetic moment with decreasing temperature.[10,11] A large localized magnetic moment of about $2.5\mu_B$ appears at Mn sites by a first-order transition,[10,12,13] accompanied by a huge positive magnetovolume effect, up to 5% in YMn_2. From the authors[4,7] this state with large localized magnetic moments at Mn sites is referred to hereafter as *a transformed phase*. Neutron diffraction experiments confirm that a transformed phase with long-range order dominates in RMn_2 compounds with $R=$ Pr,[14] Nd,[14] Gd,[15] and Y.[16–18]

Another type of magnetic state with itinerant $3d$ electrons, whose magnetic moments are induced by the rare-earth sublattice dominates in compounds with $R=$ Ho,[19] Dy,[20] Tb,[21] Er, and Tm.[2,22] No volume expansion is observed in these compounds with a small induced Mn moment ($\leqslant 1.5\mu_B$). The main feature of this induced magnetic order is that Mn spins are ordered only on sites with a strongly polarizing environment, forming a ''sandwich''-type magnetic structure with magnetic and nonmagnetic Mn layers. This magnetic state is hereafter associated with *a nontransformed phase*.

Note that the edge between transformed and nontransformed states may be easily affected, for example, by the difference in atomic packing, cubic or hexagonal, as observed in the dimorphic compound $Dy_{0.8}La_{0.2}Mn_2$.[23] The coexistence of transformed and nontransformed phases was observed in YMn_2,[13,18] $TbMn_2$,[21] and practically in all substituted systems $Tb(Mn,Fe)_2$,[9,21] $(R,Y)Mn_2$ with $R=$ Dy,[3,4,6] Ho,[5] and Tb.[7,8]

The Mn-Mn interatomic distance is one of the main factors responsible for the magnetic behavior in RMn_2 compounds. A regular change in this parameter can be realized by Mn substitution. For example, the substitution of Mn by Fe decreases Mn-Mn spacing. In the $Tb(Mn,Fe)_2$ system it allowed one to approach the region of magnetic instability from above.[9,21] In contrast, the substitution of Mn by Al increases Mn-Mn spacing, which in the $Ho(Mn,Al)_2$ allowed one approach the instability region from below.[24] However, in this system no sharp magnetovolume effect was found, suggesting that the threshold of instability was not reached.

In the present paper, we report a systematic study of the $Dy(Mn,Al)_2$ system. Mn-Mn spacing is larger in $DyMn_2$ than in $HoMn_2$. Therefore one can expect that the critical Mn-Mn distance could be reached in $Dy(Mn,Al)_2$ at lower Al substitution, allowing one to encompass the threshold of instability. To observe the evolution of magnetic and crystal structure, neutron diffraction is one of the most powerful methods.

II. EXPERIMENTAL RESULTS

Polycrystalline samples of $Dy(Mn_{1-x}Al_x)_2$ were synthesized by standard induction melting.[24] Only as-cast samples

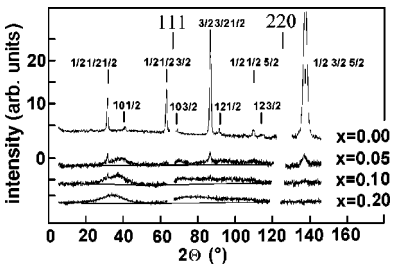

FIG. 1. The different neutron diffraction patterns of $Dy(Mn_{1-x}Al_x)_2$ measured at the diffractometer G6-1 at 10 K. The positions of nuclear Bragg reflections (the corresponding profiles are omitted) and magnetic reflections with half-integer indexes corresponding to the antiferromagnetic structure AF2 and AF3 (below) are marked by stripes.

were used in the experiments. The diffractometer G6-1 of the Laboratoire Léon Brillouin with a neutron wavelength of 4.732 Å was used to search for long-period structures. To obtain the values of the magnetic moments, additional measurements were carried out on the diffractometer DMC of the Laboratory for Neutron Scattering in Paul Scherrer Institute with a neutron wavelength of 2.559 Å. All neutron diffraction patterns were treated by the FULLPROF program.[25] The form factors for Dy^{3+} and Mn^{2+} implemented into this program were used.

In Fig. 1, the neutron diffraction patterns measured at 10 K are shown. Clearly, the character of the magnetic order drastically changes with Al substitution. It is, therefore, reasonable to consider $DyMn_2$ and the substituted compounds separately.

A. Magnetic phases in $DyMn_2$

No structural distortions from the face-centered-cubic (fcc) lattice were detected within the limits of experimental resolution. The magnetic structure at 10 K was found to be ''sandwich'' type, similar to that reported previously for $DyMn_2$,[20] $HoMn_2$,[19] and $TbMn_2$.[21] This magnetic structure has antiferromagnetic component with the propagation vector $[\frac{1}{2}\frac{1}{2}\frac{1}{2}]$ that corresponds to the second type of antiferromagnetic ordering in the fcc lattice (hereafter AF2). This component was found to be aligned close to the direction [0 1 1] at 10 K. Besides this antiferromagnetic component, the Dy moments have a ferromagnetic component of $6.1(1)\mu_B$, leading to the so-called canted antiferromagnetic structure. Mn moment has an antiferromagnetic component only. The values of the total Dy and Mn moments, their ratio, and magnetic ordering temperatures are shown in Table I. The calculated values of the magnetic moments are in good agreement with the data previously reported for the same compound.[20]

In Fig. 2(a) the temperature dependences of total moments and their ferromagnetic and antiferromagnetic components are shown. The ferromagnetic component of Dy appears below 40 K whereas the antiferromagnetic component is seen up to 50 K. It means that a collinear antiferromagnetic structure transforms to a canted one at 40 K. Below T_N, the relative intensities of magnetic reflections change with varying temperature, suggesting a rotation of the magnetic structure as a whole. From powder diffraction it is not possible to determine the direction of the ferromagnetic component. However, the profile refinement shows that the antiferromagnetic components of both Dy and Mn moments rotate continuously with decreasing temperature from the {1 1 1} plane below T_N, towards the [0 1 1] direction at 10 K.

TABLE I. Values of the ordered total moments of Dy (μ_{Dy}), Mn (μ_{Mn}) (in Bohr magnetons), their ratio and the temperatures of onset for ferromagnetic (T_N), antiferromagnetic (T_C), and short-range ordered component (T_{sro}). The estimated standard deviations are given in the brackets.

x	μ_{Dy}	μ_{Mn}	μ_{Mn}/μ_{Dy}	T_C (K)	T_N (K)	T_{sro} (K)
0	7.9(1)	1.3(2)	0.16(3)	40	50	
0.05	3.9(1)	1.6(3)	0.42(9)		45	60
0.1	1.81(15)	0.75(25)	0.41(9)		35	110

Besides the reflections with half-integer indexes that belong to the magnetic structure AF2, weak superstructure magnetic reflections were observed in the low-temperature diffraction pattern of $DyMn_2$ (Fig. 1). They can be indexed on a unit cell based on a doubling of the nuclear unit cell in one direction. The appearance of superstructure reflections is accompanied by the appearance of a weak ''shoulder'' on the left side of the nuclear reflections. The lattice parameter of 7.57(1) Å of the new phase refined from the positions of the superstructure magnetic reflections turns out to be noticeably larger than the unit-cell parameter of the main phase 7.5120(3) Å (at 10 K). From the decomposition of the nuclear reflection (2 2 0) the content of the new phase with enhanced unit cell was estimated at 5.8(2)%.

The ratio of intensities of the observed superstructure reflections corresponds to the antiferromagnetic ordering of IIIA type for the fcc lattice[26] (hereafter AF3) with the propa-

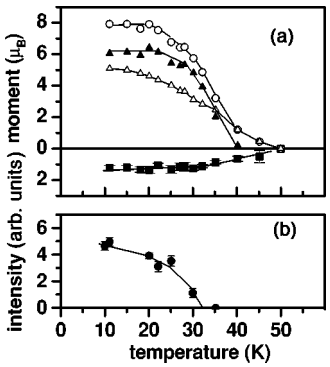

FIG. 2. (a) Temperature dependences of Mn moment (solid squares), ferromagnetic (solid triangle), and antiferromagnetic (open triangle) components of Dy moment with magnetic order AF2 in $DyMn_2$. The dependence of the total Dy moment is shown by open circles; (b) temperature dependence of the intensity of magnetic reflection $(1\ 0\ \frac{1}{2})$ from the phase with enhanced unit cell and magnetic order AF3. Errors (if not shown) do not exceed the size of symbols. The solid lines are guides for the eye.

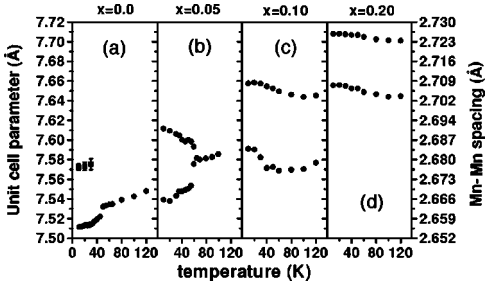

FIG. 3. Temperature dependence of the unit-cell parameters in $Dy(Mn_{1-x}Al_x)_2$. Figures (a), (b), (c), and (d) correspond to Al contents $x=0$; 0.05; 0.1, and 0.2, respectively. For $DyMn_2$ the unit-cell parameter of the phase with enlarged cell and magnetic order AF3 is shown in solid squares. Errors do not exceed the size of the symbols.

gation vector $[00\frac{1}{2}]$. In Fig. 2(b) the temperature dependence of the magnetic reflection $(10\frac{1}{2})$ is given. The magnetic order AF3 appears at a lower temperature than does the dominant order AF2. The appearance of secondary phase in $DyMn_2$ is accompanied by the positive magnetovolume effect about $\approx 1.6\%$ at the temperature of transition [Fig. 3(a)]. The negative magnetovolume effect in the main phase is due to magnetostriction.[20,19]

A weak peak attributed to intrinsic Mn moment with a magnitude of about $2.5\mu_B$ has been observed in $DyMn_2$ by nuclear magnetic resonance.[12] It is consistent with our data and confirms that in $DyMn_2$ a small amount of transformed phase with an enhanced unit cell exists due to the ordering of intrinsic Mn moments. The main nontransformed phase with AF2 structure and the secondary transformed phase with AF3 structure coexist and both exhibit long-range magnetic order.

B. Structure transformation and a coexistence of phases at substitution of Mn by Al

At small substitution $x=0.05$, the nuclear reflections show a splitting into two components below 60 K. The temperature dependence of the splitting cannot be explained by any structural distortion and points out the appearance of a new crystal phase. The change of the lattice parameters and the relative content of the two phases vs temperature are shown in Figs. 3(b) and 4(a), respectively. The structural transformation is accompanied by an abrupt change in the unit-cell parameters of the constituent phases. This transformation appears at higher temperature than the onset of long-range magnetic order [Fig. 4(b)].

The total intensity of the nuclear reflections does not change with temperature [Fig. 4(a)], indicating the absence of ferromagnetic component, while the antiferromagnetic order AF2 is still clearly seen (Fig. 1). Therefore, the observed magnetic arrangement is a collinear one. Profile refinement shows that the magnetic moments lie in the {1 1 1} planes. With decreasing temperature the relative intensities of magnetic reflections do not change, showing the absence of a spin reorientation in the substituted sample, in contrast to $DyMn_2$.

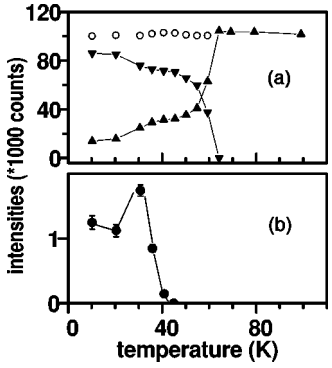

FIG. 4. (a) Temperature dependences of the intensity of the two constituents of the nuclear reflection (2 2 0) (proportional to the volumes fractions of two phases) in $Dy(Mn_{0.95}Al_{0.05})_2$. Open circles show the sum. Up and down triangles correspond to phases with enlarged and reduced unit cell, respectively. (b) Temperature dependence of the averaged intensity of magnetic reflections from AF2 structure. Errors do not exceed the size of symbols. The solid lines are guides for the eye.

Profile refinement shows that the lattice parameter of the AF2 magnetic order is exactly twice the lattice parameter of the crystal phase with the smallest unit cell. Therefore, AF2 order should be attributed to the phase with the smallest unit cell. The observed system of magnetic reflections is well approximated by a ''sandwich'' type of order with a reduced Dy moment (Table I). The pronounced maximum at 30 K in the temperature dependence [Fig. 4(b)] can be readily understood assuming that with cooling the magnetic moment increases whereas the volume fraction of the phase decreases (Fig. 4). The observed negative magnetovolume effect in this phase is due to magnetostriction as in $DyMn_2$. Therefore, the phase with a smaller unit cell is identified as a nontransformed one.

The observed negative magnetovolume effect in substituted sample is similar to that observed in $DyMn_2$. Interestingly, this effect is much stronger for $x=0.05$ than for $x=0$, suggesting to attribute it not only to magnetostriction, as in $DyMn_2$, but to a segregation process induced by magnetism. Namely, in the substituted compound, the transition towards the transformed phase would occur preferentially in regions with a higher Al content, hence with a larger lattice parameter. The part of the sample remaining in the nontransformed phase would, therefore, have a slightly smaller Al content. This self-segregation process could be favored by the statistical fluctuations of concentrations always present in the substituted compounds.

Besides the magnetic Bragg reflections a strong diffuse magnetic scattering appears in $Dy(Mn_{0.95}Al_{0.05})_2$ (Fig. 5). Two types of diffuse scattering can be distinguished below the structural transition at 60 K. First, a diffuse scattering, which transforms into the Bragg reflections with decreasing temperature. This scattering based on AF2 structure should be attributed to short-range spin correlations, precluding the onset of the long-range magnetic order AF2 and will not be discussed further.

In addition to the latter, diffuse maxima around the nods of primitive lattice appear. They can be well approximated

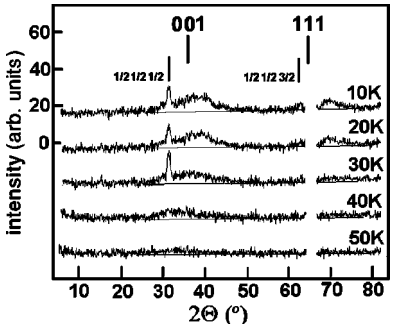

FIG. 5. Evolution of the diffuse magnetic scattering in $Dy(Mn_{0.95}Al_{0.05})_2$.

by a set of Bragg peaks, broadened by the ''finite size'' effect. The unit-cell parameter of the primitive magnetic lattice calculated from the positions of the diffuse peaks practically coincides with the unit-cell parameter of the transformed phase with expanded lattice. Therefore, this diffuse scattering should be attributed to the phase with expanded lattice. The observed expansion of the unit-cell volume of 2% (with respect to the nontransformed phase at 60 K) is in agreement with the magnetovolume expansion known for the transformed phases in RMn_2 compounds.[1] Thus, a nontransformed phase with a long-range magnetic order AF2 and a transformed phase with short-range order coexist at low temperatures in $Dy(Mn_{0.95}Al_{0.05})_2$.

In contrast to $Dy(Mn_{0.95}Al_{0.05})_2$, samples with higher Al contents $x=0.1-0.2$ are initially composed (already at room temperature) of two crystal phases (Fig. 3). Profile refinement shows that the lattice parameter and Al content differ in both phases, as in $Ho(Mn,Al)_2$.[24] The volume fractions of the phases with smaller and larger unit-cell parameter weakly depend on the nominal concentration and are estimated to about 17 and 83 vol. %, respectively. The long-range AF2 order is practically suppressed in these samples, and the diffuse scattering around the nodes of the primitive lattice persists alone.

C. Peculiarities of the diffuse scattering

A strong diffuse scattering is observed in all substituted samples. It appears at higher temperatures when Al content increases (Table I) around the nodes of primitive cubic lattice and cannot be associated with any known type of antiferromagnetic order in fcc lattice. This scattering has been associated with an expanded lattice in $Dy(Mn_{0.95}Al_{0.05})_2$ and has important features.

First, this diffuse scattering increases with decreasing temperature and at some temperature becomes constant. For example, at $x=0.05$, it becomes temperature independent below about 20 K (Fig. 5). This can be understood assuming that short-range magnetic correlations corresponds to some ground state of the system.

Second, the scattering has general structural peculiarities. We consider the broad maxima as a manifestation of the short-range magnetic order in some ''clusters'' of finite size. An evaluation of the correlation length by the Scherrer formula yields a value of about 20 Å, as in $Ho(Mn,Al)_2$. The correlation length practically does not depend on temperature and slightly increases with increasing Al concentration.

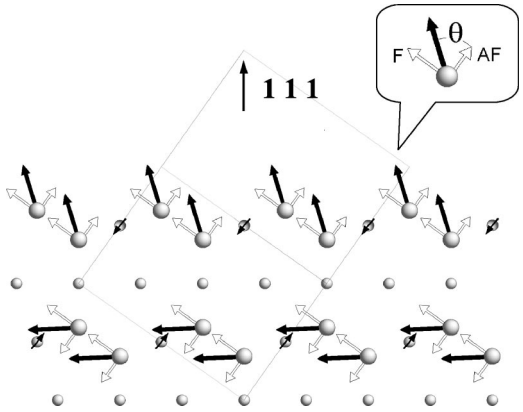

FIG. 6. Projection of the canted magnetic structure of $DyMn_2$ on $(1\bar{1}0)$ plane. Dy and Mn atoms are shown by large and small spheres, respectively. Solid arrows define the magnetic moment direction, open arrows are ferromagnetic (F) and antiferromagnetic (AF) components (see text). Dotted line shows the projection of the unit cell.

The relative intensities of diffuse peaks change with substitution, but their positions always correspond to a single lattice. Therefore, one can estimate the unit-cell parameter of the latter. At $x=0.05$ this parameter was found to be close to the unit-cell parameter of the expanded crystal phase in the transformed state. It allows us to associate the observed diffuse scattering with a short-range ordering of spontaneous Mn moments. However, at higher substitutions the unit-cell parameter of the primitive magnetic lattice is enlarged. For example, in $Dy(Mn_{0.9}Al_{0.1})_2$ this parameter at 10 K was estimated as 7.76(2) Å, well above the unit-cell parameters of the constituent crystal phases 7.591(2) Å and 7.6574(6) Å. It suggests that at higher substitution magnetic correlations tend to form a lattice, which becomes incommensurate with the nuclear one.

III. DISCUSSION

A. Exchange interaction in the "sandwich" model

We now analyze the ''sandwich'' type of antiferromagnetic structure AF2 with magnetic and nonmagnetic Mn layers taking into account nearest-neighbor exchange interactions only. In Fig. 6 the orthographic projection of magnetic structure observed in $DyMn_2$ is shown. No ferromagnetic component of Mn spin was detected in experiment, so we assume a collinear Mn sublattice.

Each R atom has three nearest R neighbors in the same plane with parallel moments and one neighbor in another plane, separated by a layer of nonmagnetic Mn atoms. Each R atom has three nearest Mn neighbors. Each Mn atom has six nearest R neighbors from the same double layer, six Mn neighbors from the same double layer with parallel moments and six Mn neighbors from the nearest double layers with antiparallel moments. The free energy written within the frame of Heisenberg model is given as follows:

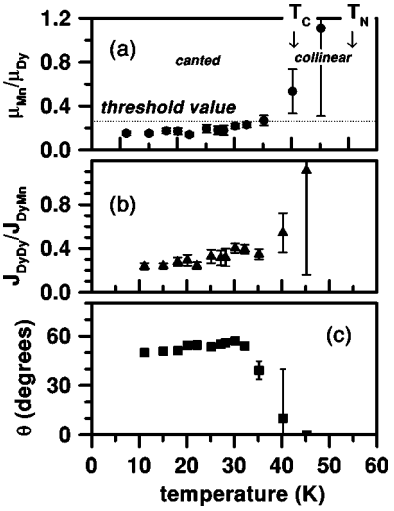

FIG. 7. $DyMn_2$. Temperature dependences: (a) the ratio of magnetic moments μ_{Mn}/μ_{Dy}; (b) the ratio of effective exchange constants of interactions J_{DyDy}/J_{DyMn}, (c) angle of canting θ.

$$E=-J_{RR}M_R^2(3-\cos 2\theta)+6J_{RMn}M_RM_{Mn}\cos\theta, \quad (1)$$

where M_R and M_{Mn} are the values of R and Mn moments, J_{RR} and J_{RMn} are the effective exchange constants of R-R and R-Mn interactions, respectively. Mn-Mn interactions cancel owing to the symmetry of the magnetic structure. The parameter θ defines the canting

$$\cos\theta=M_{RA}/M_R \quad (2)$$

Here M_{RA} is the antiferromagnetic component of the total moment M_R (inset in Fig. 6). The energy (1) can be minimized with respect to θ, which leads to three possible solutions: (1) a collinear structure with antiparallel R and Mn moments ($\theta=0$); (2) a collinear structure with parallel R and Mn moments ($\theta=\pi$), and (3) a canted structure with $\theta=\theta_0$, which corresponds to the condition

$$\cos\theta_0=-\frac{3g}{4}\frac{\mu_{Mn}}{\mu_R}\frac{J_{RMn}}{J_{RR}}, \quad (3)$$

here μ_{Mn} and μ_R are the magnetic moments of Mn and R, respectively and g is the Landé factor.

We use classical equations to analyze our data, taking into account the temperature by the thermal variations of μ_{Mn}, μ_R and angle θ as parameters calculated from experimental data (Fig. 7). The ratio J_{RR}/J_{RMn} calculated from Eq. (3) and shown in Fig. 7(b) remains constant within the accuracy of the measurements in the canted phase, confirming that the proposed model is close to reality. The average ratio was evaluated as 0.26(1).

It is easy to see by comparing the energies of the different solutions that canted structure is stable with respect to a collinear structure at the condition

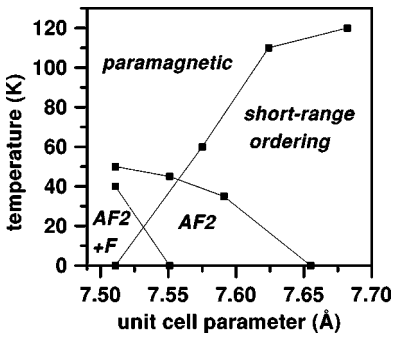

FIG. 8. Phase diagram for system $Dy(Mn_{1-x}Al_x)_2$. AF2+F and AF2 refer to ordered canted antiferromagnetic and collinear antiferromagnetic phases, respectively.

$$\cos\theta_0<1 \text{ or } \frac{\mu_{Mn}}{\mu_R}<\frac{4}{3g}\left|\frac{J_{RR}}{J_{RMn}}\right|. \quad (4)$$

Since for ion Dy^{3+} $g=4/3$, it is natural to consider that the threshold value of μ_{Mn}/μ_{Dy} is equal to the calculated averaged ratio $|J_{RR}/J_{RMn}|$. Above this value either ferromagnetic ($J_{RMn}>0$) or antiferromagnetic ($J_{RMn}<0$) alignment of Mn and Dy moments should be stable. The ratio μ_{Mn}/μ_R increases as the temperature increases, so that a canted structure is destabilized to the benefit of a collinear one [Fig. 7(a)].

At small substitution $x=0.05$ T_N decreases from 50 K to about 45 K (Table I). Therefore, exchange interactions are not strongly affected. In Table I we see that for the canted phase of $DyMn_2$ the ratio $\mu_{Mn}/\mu_R=0.16(3)$ is lower than the threshold value 0.26(1), while in the substituted compound with a stable collinear order this ratio reaches a much larger value 0.4(1). The destabilization of a canted structure at small Al substitution could be explained by the decrease of the ordered Dy moment and increase of ratio μ_{Mn}/μ_R, while J_{RR}/J_{RMn} changes weakly.

The transformation of a canted antiferromagnetic structure to a collinear one was observed in the systems $(Dy,Y)Mn_2$ (Ref. 4) and $(Ho,Y)Mn_2$.[5] We calculated J_{RR}/J_{RMn} in the frame of the proposed model from the data reported.[4,5] The value J_{RR}/J_{RMn} for $DyMn_2$ was estimated as 0.24(2), in a good agreement with our estimation. For $HoMn_2$ the calculated ratio turns out to be 0.17(7).

B. Effects of substitution

The magnetic phase diagram of $Dy(Mn_{1-x}Al_x)_2$ is given in Fig. 8. With lattice constant increases, the long-range AF2 order transforms from canted to collinear one. Together with the strong suppression of the long-range antiferromagnetic order, the substitution yields the appearance of short-range magnetic order, driven by spontaneous, intrinsic Mn spins. With increasing Al content T_N decreases while T_{sro} strongly increases. This increase is directly connected with the increase of Mn-Mn spacing and the corresponding increase of spontaneous Mn spins.

It is well known that a magnetovolume effect is a result of localization of Mn moment. Obviously, the Mn-Mn spacing in $Dy(Mn_{0.95}Al_{0.05})_2$ when this effect is maximal can be considered as critical distance in the system $Dy(Mn,Al)_2$. The calculated value of 2.578 Å differs from 2.665 Å and 2.663 Å reported for $(Dy,Y)Mn_2$ and $(Ho,Y)Mn_2$.[4,5] It means that the concept of a unique critical distance cannot be rigorously valid among all substituted systems with frustrated Mn-Mn bonds. Nevertheless this concept, postulating that the greater the Mn-Mn distance the more stable the intrinsic Mn magnetism, can be used for qualitative consideration.

In fact, our studies show that the content of the transformed phase increases with increasing substitution and Mn-Mn spacing. In $DyMn_2$ the transformed phase appears only in 5.8(2)% of the sample, while at $x=0.05$ the amount of transformed phase reaches 90%. The increase of T_{sro} confirms the increase of spontaneous Mn moment in a disordered state. The disappearance of long-range order and appearance of short-range order result from the weak *R-R* exchange interaction and the increasing role of the frustrated Mn sublattice in the formation of the magnetic state.

Transformed and nontransformed phases both with long-range order coexist at low temperatures in $TbMn_2$ and $Tb(Mn,Fe)_2$,[9,21] similar to observed in $DyMn_2$. The coexistence of transformed and nontransformed phases with short-range order was found in $(Tb,Y)Mn_2$ (Refs. 7,8) as well as in Y-substituted systems $(Dy,Y)Mn_2$ (Ref. 4) and $(Ho,Y)Mn_2$.[5] A similar behavior was observed in $Dy(Mn_{0.95}Al_{0.05})_2$. The transformed phase shows short-range order while a nontransformed state remains paramagnetic in the narrow temperature interval 45–60 K, below the long-range magnetic order AF2 develops.[27]

IV. CONCLUSION

Neutron diffraction study of the $Dy(Mn_{1-x}Al_x)_2$ system shows that with substituting Mn by Al this system encompasses the region of magnetic instability. Transformed and nontransformed phases with intrinsic and induced Mn moments, respectively, coexist at small substitution. In $DyMn_2$ a small amount ($\approx 5\%$) of the transformed phase with the ordered intrinsic Mn spins was detected while in $Dy(Mn_{0.95}Al_{0.05})_2$ the amount of the transformed phase increases to 90%. However, in the last case only short-range magnetic order is observed in the transformed phase. When Al content increases further the long-range order of Dy and induced Mn moments is progressively suppressed while a short-range magnetic order of intrinsic Mn spins develops.

A small substitution destroys the ferromagnetic component of Dy moment and the long-range magnetic order transforms from a canted to a collinear one. This transformation can be well described using Heisenberg model with nearest neighbors applied to the ''sandwich'' type of magnetic order with nonmagnetic Mn layers. From the experimental data for $DyMn_2$, the ratio of the Dy-Dy and Dy-Mn interactions J_{RR}/J_{RMn} was estimated at 0.26(1).

ACKNOWLEDGMENTS

This work was supported by Grants of RFBR (N-99-02-17273 and N-00-02-17844), and the Russian Federal Foundation for Neutron Studies on Condensed Matter. One of us (I.V.G.) acknowledges the financial support of C.N.R.S. during his stay in LLB.

[1] M. Shiga, Physica B **149**, 293 (1988).
[2] M. Shiga, J. Magn. Magn. Mater. **129**, 17 (1994).
[3] C. Ritter, S. Mondal, S.H. Kilcoyne, R. Cywinski, and B. Rainford, J. Magn. Magn. Mater. **104-107**, 1427 (1992).
[4] C. Ritter, R. Cywinski, S.H. Kilcoyne, S. Mondal, and B. Rainford, Phys. Rev. B **50**, 9894 (1994).
[5] C. Ritter, R. Cywinski, and S.H. Kilcoyne, Z. Naturforsch., A: Phys. Sci. **50**, 191 (1995).
[6] C. Ritter, C. Marquina, and M.R. Ibarra, J. Magn. Magn. Mater. **151**, 59 (1995).
[7] J. De Teresa, M.R. Ibarra, C. Ritter, C. Marquina, Z. Arnold, and A. del Moral, J. Phys.: Condens. Matter **7**, 5643 (1995).
[8] J.M. De Teresa, C. Ritter, M.R. Ibarra, Z. Arnold, C. Marquina, and A. del Moral, J. Phys.: Condens. Matter **8**, 8385 (1996).
[9] S. Mondal, S. Kilcoyne, B. Rainford, and R. Cywinski, Physica B **180-181**, 111 (1992).
[10] Y. Nakamura, M. Shiga, and S. Kawano, Physica B **120**, 212 (1983).
[11] H. Wada, H. Nakamura, K. Yoshima, M. Shiga, and Y. Nakamura, J. Magn. Magn. Mater. **70**, 134 (1987).
[12] K. Yoshimura, M. Shiga, and Y. Nakamura, J. Phys. Soc. Jpn. **55**, 3585 (1986).
[13] I. Yu. Gaidukova and A.S. Markosyan, Phys. Met. Metallogr. **54**, 168 (1982).
[14] R. Ballou, J. Deportes, R. Lemaire, and B. Ouladdiaf, J. Appl. Phys. **63**, 3487 (1988).
[15] B. Ouladdiaf, C. Ritter, R. Ballou, and J. Deportes, Physica B **276-278**, 670 (2000).
[16] R. Ballou, J. Deportes, R. Lemaire, Y. Nakamura, and B. Ouladdiaf, J. Magn. Magn. Mater. **70**, 129-133 (1987).
[17] T. Freltoft, P. Boni, G. Shirane, and K. Motoya, Phys. Rev. B **37**, 3454 (1988).
[18] R. Cywinski, S.H. Kilcoyne, and C. Scott, J. Phys.: Condens. Matter **3**, 6473 (1991).
[19] C. Ritter, R. Cywinski, S.H. Kilcoyne, and S. Mondal, J. Phys.: Condens. Matter **4**, 1559 (1992).
[20] C. Ritter, S.H. Kilcoyne, and R. Cywinski, J. Phys.: Condens. Matter **3**, 727 (1991).
[21] P. Brown, B. Ouladdiaf, R. Ballou, J. Deportes, and A.S. Markosyan, J. Phys.: Condens. Matter **4**, 1103 (1992).
[22] G.P. Felcher, L.M. Corliss, and J.M. Hastings, J. Appl. Phys. **36**, 1001 (1965).

[23] B. Ouladdiaf, R. Ballou, J. Deportes, and E. Lelievre-Berna, J. Magn. Magn. Mater. **140-144**, 1811 (1995).
[24] I.S. Dubenko, I.V. Golosovsky, A.S. Markosyan, and I. Mirebeau, J. Phys.: Condens. Matter **10**, 11 755 (1998).
[25] J. Rodriguez-Carvajal, the computer code FULLPROF (LLB, Saclay, France, 2000).
[26] Yu.A. Izyumov, V. E. Naish, and R. P. Ozerov, *Neutron Diffraction of Magnetic Materials* (Plenum, New York, 1991).
[27] M. Shiga, H. Wada, Y. Nakamura, and K. Yoshimura, J. Magn. Magn. Mater. **54-57**, 1073 (1986).